Gd contents, mechanical and corrosion properties of Mg–10Gd–3Y–0.5Zr alloy purified by fluxes containing GdCl$_3$ additions

Wei Wang [a,b], Guohua Wu [a,b,*], Qudong Wang [a,b], Yuguang Huang [a,b], Wenjiang Ding [a,b]

[a] National Engineering Research Center of Light Alloy Net Forming, Shanghai Jiao Tong University, 800 Dongchuan Road, Shanghai 200240, China

[b] State Key Laboratory of Metal Matrix Composites, Shanghai Jiao Tong University, Shanghai 200240, China

ABSTRACT

The effects of GdCl$_3$ in flux on the loss of Gd, microstructure, mechanical and corrosion properties of Mg–10 wt.% Gd–3 wt.% Y–0.5 wt.% Zr (GW103K) alloy were investigated. The results indicate that the loss of Gd in the alloy decreased when the melts were refined by fluxes containing GdCl$_3$ additions. Thermodynamic analysis revealed that the decline of Gibbs free energy is the main reason, which slows down the reaction rate between MgCl$_2$ and Gd in melts. In as-cast condition, after treated with 5 wt.% GdCl$_3$ additions, tensile yield strength, ultimate tensile strength and elongation of the alloy could reach the peak value of 201.51 MPa, 154.68 MPa and 2.56% respectively. 5 wt.% NaCl aqueous solution immersion test shows that the corrosion rate of GW103K alloy decreased to 0.437 mg cm^{-2} d^{-1} after refined by JDMJ + 5 wt.% GdCl$_3$. However GdCl$_3$ additions have no effects on microstructure and fracture pattern of GW103K alloy.

© 2008 Elsevier B.V. All rights reserved.

1. Introduction

Magnesium alloys containing heavy rare earth (RE) elements have a high strength-to-weight ratio and Mg–Gd–Y–Zr series alloys, such as Mg–10 wt.% Gd–3 wt.% Y–0.5 wt.% Zr (GW103K) alloy, show large promise for the automotive industry because of its higher specific strength at both room and elevated temperature and good creep resistance than commercially available magnesium alloys [1–5]. However, magnesium and rare earth elements tend to oxidize rapidly in air during the course of smelting due to their high chemical activities, which results in burn loss of expensive rare earth elements and formation of nonmetallic inclusions [6]. As to GW103K alloy, the burn loss of Gd fluctuate the compositions and bring difficulty to fabricate the alloy. The oxide inclusions destroy the continuity of the magnesium matrix, induce the defects such as pores and cracks, and hence impair the mechanical and corrosion properties of the alloy [7]. Therefore, in order to improve the mechanical and corrosion properties of GW103K alloy, it is important to find a new purification method to control the Gd loss and the content of nonmetallic inclusions. The lack of efficient purification methods currently limits the application of GW103K alloy.

It is well known that MgO is the main nonmetallic inclusions in Mg alloy. Liquid MgCl$_2$ has an excellent adsorption capability to MgO inclusions and forms MgCl$_2$·5MgO compound which sinks to the bottom of crucible. This is the reason why MgCl$_2$ is widely accepted as one of the main ingredients in flux. Accordingly, traditional flux refining has still been considered as one of the most efficient methods to remove nonmetallic inclusions in magnesium alloys. However, rare earth elements, such as Gd in GW103K alloy, tend to react with MgCl$_2$ and result in the loss of Gd. Although fluxes without MgCl$_2$ were employed to refine rare earth magnesium alloys for the purpose of reducing the loss of RE elements, such MgCl$_2$-free fluxes are not very efficient in removing the nonmetallic inclusions [8]. Therefore, it is an urgent task to find new methods to refine GW103K alloy.

With the aim to achieve both the high refining efficiency and suppressing the loss of Gd, in the present work a new flux containing GdCl$_3$ additions specially for refining GW103K alloy was developed. Meanwhile, the refining process with this new flux is supposed to be more economical than the process with normal commercial flux. The reason lies in two aspects: one is that GdCl$_3$ represents an affordable source of Gd that is also relatively to obtain; the other is that the extra Gd loss induced by fabricating Mg–Gd master alloy could be avoid. In this work, the effects

* Corresponding author at: National Engineering Research Center of Light Alloy Net Forming, School of Materials Science & Engineering, Shanghai Jiao Tong University, 800 Dongchuan Road, Shanghai 200240, China. Tel.: +86 21 54742630; fax: +86 21 34202794.

E-mail addresses: ghwu@sjtu.edu.cn, ghwu@hotmail.com (G. Wu).

Table 1
Compositions of the fluxes (wt.%).

Flux	Composition	
	JDMJ	GdCl₃
JDMJ	100	0
JDMJ + 5% GdCl₃	95	5
JDMJ + 10% GdCl₃	90	10

of GdCl₃ additions on the loss of Gd were studied and the mechanism was illuminated by thermodynamic calculation. Moreover, the influences of GdCl₃ additions on the microstructure, mechanical properties and the corrosion resistance of GW103K were investigated as well.

2. Materials and experimental procedure

2.1. Materials

Analytically pure GdCl₃ was added into a flux named JDMJ and mixed in QM-ISP pebble mill for 3 h. Then the new flux was added into the melt for refining purpose. The ingredients of the new fluxes were listed in Table 1, where JDMJ flux (wt.%, $MgCl_2$: 45, KCl: 25, NaCl: 20, $CaCO_3$: 10) was developed by Shanghai Jiao Tong University [9]. GW103K alloy were fabricated by pure Mg ingots and Mg–25 wt.% Gd, Mg–25 wt.% Y, Mg–30 wt.% Zr master alloys.

2.2. Smelting and refining

Before smelting, Mg ingots, master alloys, fluxes and tools used in the experiments were heated to 200 °C in a baking oven in order to eliminate water. Smelting was performed in a 7 kW crucible electric resistance furnace under protection of a shield gas consisting of SF_6 (1 vol.%) and CO_2 (bal.). 2.5 wt.% (ratio to the whole raw metal) new fluxes were added to refine the melt at 760 °C. After refining, the melt was held about 30–45 min, and then, at 740 °C, poured into the metallic molds preheated to 400 °C.

2.3. Mechanical properties tests

In order to obtain dense specimens, all the tensile specimens were cut from the bottom of the ingots. The gage dimension of the specimens is 54.5 mm × 15 mm × 2 mm. The ambient temperature tensile tests were carried out on a Zwick/Roell materials testing machine at a crosshead speed of 0.5 mm min⁻¹. Three specimens under the same condition were tested and the final values were obtained in term of their average value. Owing to the high strength of GW103K alloy exhibited in the T6 heat treatment condition, the mechanical properties and corrosion resistance were investigated in present work in the T6 condition as well. T6 heat treatment method is: solution treatment at 500 °C for 8 h in argon atmosphere, peak-ageing at 225 °C in an oil bath for 16 h.

2.4. Compositions determination and microstructure observation

Metallic powders for chemical compositions determination were drilled from different sections of five ingots which were fabricated by the same heat and then mixed homogeneously. Subsequently, the chemical compositions of the alloy were determined by inductively coupled plasma atomic emission spectroscopy (ICP-AES). The morphologies of inclusions in alloys and general microstructure observations were performed by optical microscopy (OM) and field emission scanning electron microscope (FESEM). The composition of inclusions were analyzed by energy dispersive spectroscope (EDS) attached to the SEM. The phase

composition of the alloy was studied by X-ray diffraction (XRD) technique.

2.5. Corrosion resistance

The size of specimens for immersion corrosion test was 35 mm (diameter) × 4 mm (thickness). The specimens were polished successively on fine grades of emery papers up to 800 grit. The greasy dirt on the surface was cleaned in ethanol and acetone and dried by warm flowing air. After that, the total surface area (SA in cm²) and weight (W_0 in mg) of the specimens should be measured. The specimens were immersed in a 5 wt.% NaCl aqueous solution (pH 8.3) at room temperature (25 ± 0.5 °C). After three days immersion (immersion time, EP), the specimens were taken out and cleaned in a solution of 15% Cr_2O_3 + 1% $AgNO_3$ in 500 ml water at boiling condition for about 5 min. Following that the specimens were rinsed by distilled water and dried by warm air. The weight of the corroded specimen (W_c in mg) was measured by an analytical balance. Then the weight loss (W_L in mg) and the corrosion rate (CR in mg cm⁻² d⁻¹) could be calculated by the following equations:

$$W_L = W_0 - W_c$$

$$CR = \frac{W_L}{SA \times EP}$$

2.6. Potentiodynamic polarization curve

Electrochemical polarization tests were carried out in a corrosion cell containing 200 ml of 5 wt.% NaCl using a standard three electrode configuration: saturated calomel as a reference with a stainless steel electrode as counter and the sample as the working electrode. A ZF-10 measurement system was used. Specimens were immersed in the test solution and a polarization scan was carried out at a rate of 1 mV s⁻¹, after allowing a steady state potential to develop.

3. Results and discussion

3.1. RE concentration

Fig. 1 shows the relationship between the loss of Gd in alloy and GdCl₃ additions during the refining process. The results indicate that, with the increase of GdCl₃ additions, the loss of Gd decreased
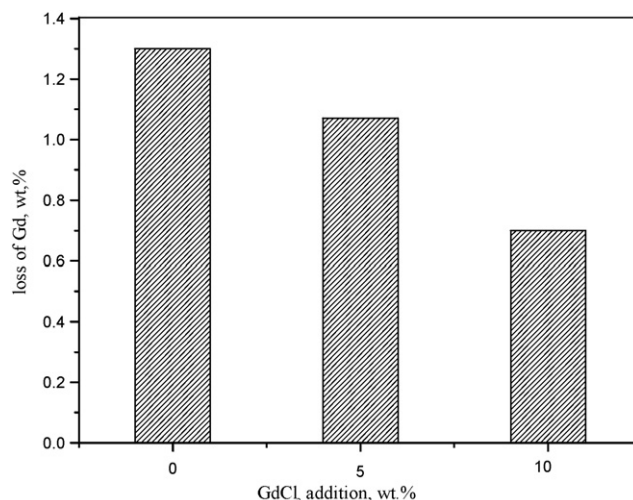

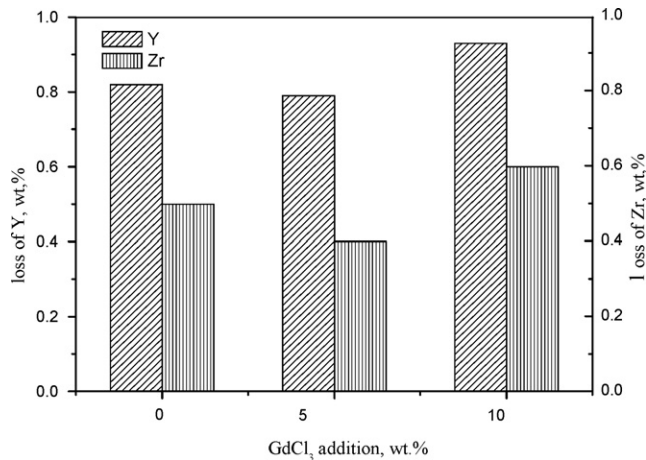**Fig. 1.** Effects of GdCl₃ additions on the loss of Gd.

Fig. 2. Effects of GdCl$_3$ additions on the loss of Y and Zr.

Fig. 4. Effects of different treatments on the corrosion rates of GW103K alloy.

directly. Actually, the Gd loss could be limited to 0.7 wt.% when the GW103K alloy purified by JDMJ + 10 wt.% GdCl$_3$ additions. This is much lower than the specimen purified by pure JDMJ flux (1.3 wt.% Gd loss). Even when refined by JDMJ + 5 wt.% GdCl$_3$ additions, the Gd loss is only 1.07 wt.%. This means that the loss of Gd in alloy could be suppressed to a certain degree when refined by the fluxes with GdCl$_3$ additions.

The losses of Y and Zr in alloy were also investigated. The results (Fig. 2) indicate that the fluxes containing GdCl$_3$ additions have no obvious influence on the loss of Y and Zr. The loss of Y kept at about 0.8 wt.% and the loss of Zr remained within 0.4–0.6 wt.%.

3.2. Mechanical properties

In order to exhibit the purifying effectiveness, unrefined specimens were taken before refining by any flux. Fig. 3 shows the effects of GdCl$_3$ contents on mechanical properties of GW103K alloy. In as-cast condition, the relationship between the ambient temperature mechanical properties and the GdCl$_3$ contents is shown in Fig. 3a. Initially, the ultimate tensile strength (σ_b), yield strength at 0.2% offset (σ_s) were improved with the increasing of GdCl$_3$ in fluxes. Compared with the unrefined specimens, when GdCl$_3$ additions increased to 5 wt.%, the σ_b, σ_s improved from 131.67 MPa, 108.35 MPa to peak value 201.51 MPa, 154.68 MPa by 53% and 42.7%, respectively. For the specimens refined only by pure JDMJ flux, the σ_b and σ_s reached 189.5 MPa and 141.91 MPa, which are higher than the unrefined specimens but still lower than those purified with 5 wt.% GdCl$_3$ additions. Moreover, the elongation of the alloy (δ) treated by fluxes containing GdCl$_3$ additions was improved signif-
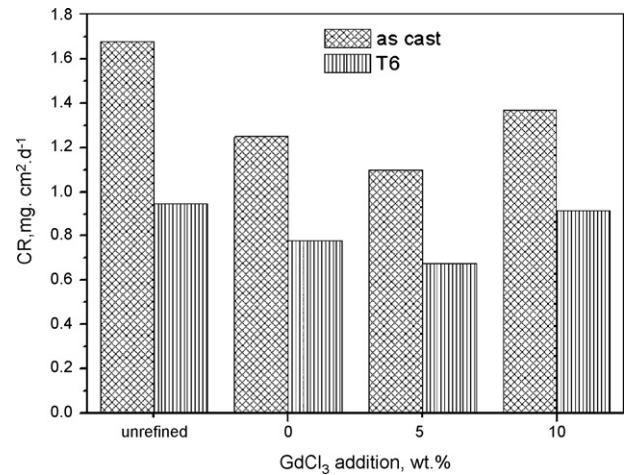
icantly. The elongation attained the highest value of 2.56% when GdCl$_3$ additions was 5 wt.%. While for the unrefined specimen and a specimen refined with pure JDMJ, the elongation reached only 0.13% and 1.51%, respectively. Keeping on increasing GdCl$_3$ content to 10 wt.%, the σ_b, σ_s and δ decreased contrarily to 175.6 MPa, 152.98 MPa and 0.51%.

In the T6 condition, the mechanical properties were similar to those in the as-cast condition (Fig. 3b). In comparison to unrefined and pure JDMJ refined specimens, the best combination of tensile properties (σ_b, σ_s and δ) was achieved with the 5 wt.% GdCl$_3$ additions. σ_b, σ_s and δ reach 311.12 MPa, 241.17 MPa and 1.53% respectively. However, the mechanical properties declined when the GdCl$_3$ additions increased at 10 wt.%.

In general, whether in as-cast or T6 condition, the mechanical properties of GW103K declined in the following sequence: JDMJ + 5 wt.% GdCl$_3$ additions > JDMJ + 10 wt.% GdCl$_3$ additions > JDMJ > unrefined.

3.3. Corrosion resistance

The corrosion rates of GW103K alloy treated with different refining processes are shown in Fig. 4. The corrosion rates decreased in following order: no refining > pure JDMJ > JDMJ + 10 wt.% GdCl$_3$ additions > JDMJ + 5 wt.% GdCl$_3$ additions. The order also fit the trend of specimens in T6 condition. In as-cast condition, compared with unrefined specimens, the corrosion rate of the specimens treated by 5 wt.% GdCl$_3$ additions decreased dramatically from 1.68 mg cm^{-2} d^{-1} to 1.1 mg cm^{-2} d^{-1} by 34.5%. Fig. 5 shows the mor-
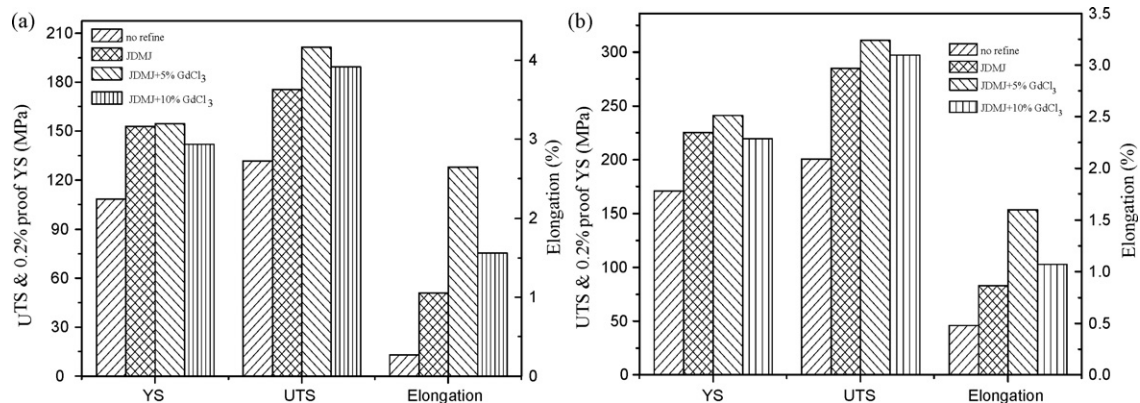

Fig. 3. Effects of GdCl$_3$ additions on the mechanical properties of GW103K alloy (a. as-cast condition, b. T6 condition).
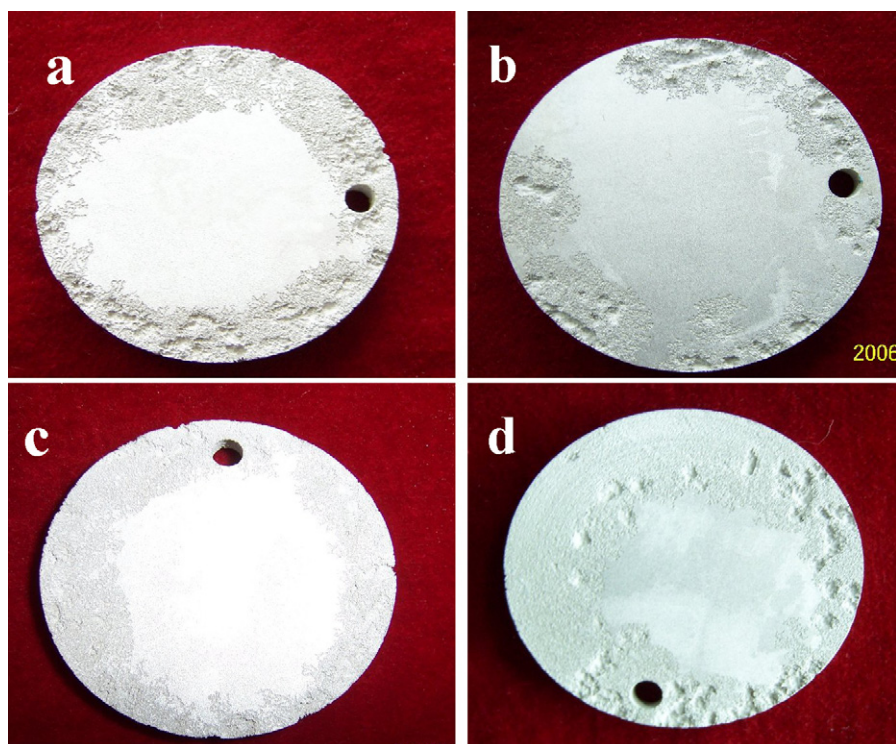
Fig. 5. Surface corrosion morphologies of GW103K alloy after immersed in 5 wt.% NaCl aqueous solution for 3 days (a. unrefined, b. refined by JDMJ, c. refined by JDMJ + 5 wt.% GdCl$_3$ additions, d. refined by JDMJ + 10 wt.% GdCl$_3$ additions).

phological characteristics of the corroded surfaces of the specimens immersed in 5 wt.% NaCl aqueous solution for 3 days, where (a), (b), (c) and (d) represent the samples treated with different refining processes. Deep corrosion pits were distributed on the surface, except for the one refined with 5 wt.% GdCl$_3$ additions (Fig. 5c). The deleterious effects of nonmetallic inclusions on corrosion resistance of magnesium alloys can be attributed to the forming of galvanic coupling between the nonmetallic inclusions and magnesium matrix [10], which then accelerates the corrosion rate. The specimens refined with 5 wt.% GdCl$_3$ additions exhibit excellent corrosion resistance because of its remarkable ability of removing nonmetallic inclusions. This reduction of nonmetallic inclusions decreases the cathode areas and thus improves the corrosion resistance of the alloy. However, when GdCl$_3$ increased to 10 wt.%, more flux remained in the melt and formed flux inclusions at the same time. These flux inclusions are mainly chlorides, and greatly accelerate the electrochemical corrosion process on the contrary.

The potentiodynamic polarization curves of GW103K alloy purified by fluxes containing different GdCl$_3$ contents are shown in Fig. 6. It can be seen that the polarization curves for all the specimens are not symmetrical between their anodic and cathodic branches. Much sharper changes in log I versus applied potential were observed in the anodic polarization branches than in the cathodic polarization branches. And the corrosion potential increases in the following order: pure JDMJ < JDMJ + 10 wt.% GdCl$_3$ additions < JDMJ + 5 wt.% GdCl$_3$ additions. Furthermore, the cathodic current density is higher for specimens refined by JDMJ + 5 wt.% GdCl$_3$ additions than others at all potentials. All the differences are owing to the different nonmetallic inclusion contents in the alloy refined by the flux with different GdCl$_3$ additions.

For the specimens in T6 condition, although the tendency is similar, the corrosion rates are generally lower than that of in as-cast condition (see Fig. 4). This can be explained via the phase composition change of the alloy under different heat treatment conditions. Fig. 7 shows that GW103K alloy is constituted of α-Mg matrix and
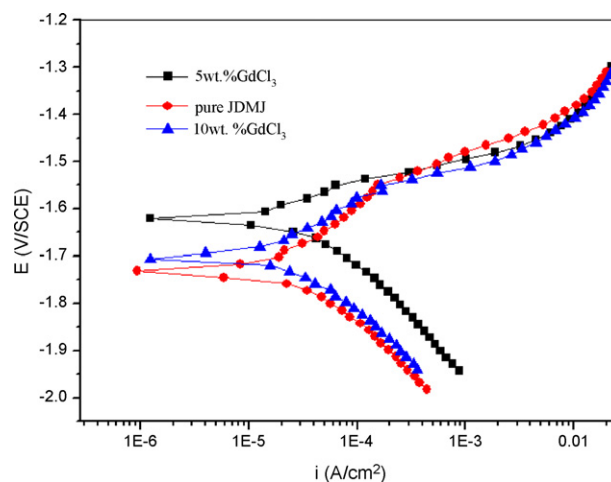

Fig. 6. Polarization curves of GW103K alloy.

a network of the eutectic phase in as-cast condition. In the T6 condition, most of the eutectic phases have dissolved into the matrix (Fig. 8). It was reported [11] that the eutectic phase acted as cathode and forms galvanic coupling corrosion with the Mg matrix, and then speeds up the corrosion process of the alloy. The decrease in the volume fraction of the eutectic phase in the T6 condition enhances the corrosion resistance.

3.4. Ingredients, morphologies and contents of inclusions

It can be seen from Fig. 9 that the largest inclusions in GW103K alloy exhibit spherical, bar-shape and irregular morphology. In addition to these large inclusions, some fine inclusions were dispersed within grains and on the grain boundary. These inclusions cut off the continuity of the matrix, cause stress constrain, supply
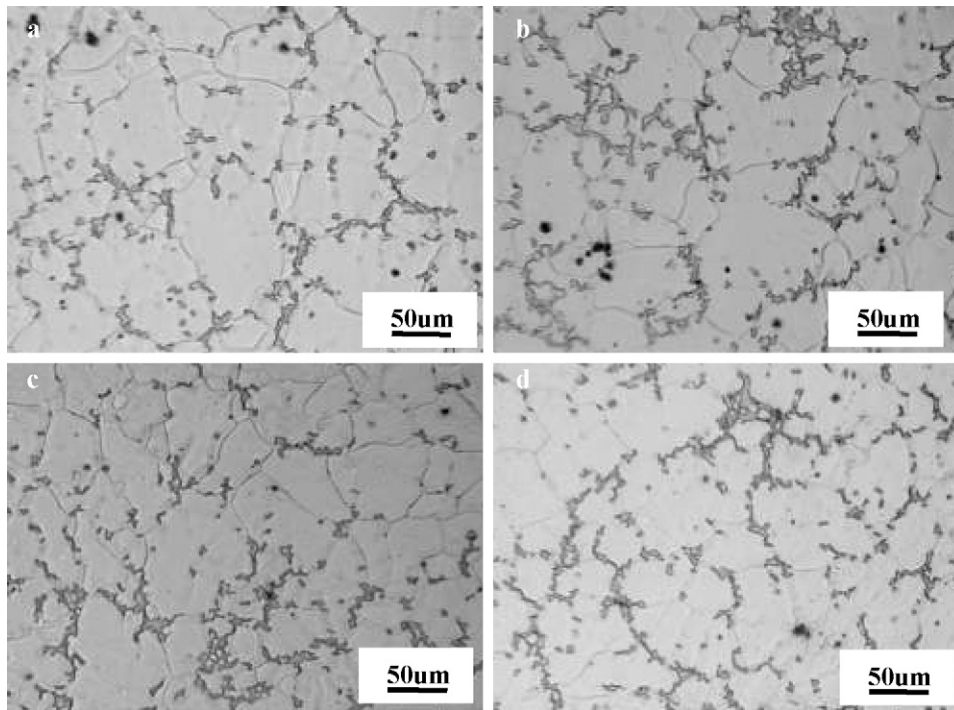
Fig. 7. Microstructures of GW103K alloy refined by different treatments (a. unrefined, b. refined by JDMJ, c. refined by JDMJ + 5 wt.% GdCl$_3$ additions, d. refined by JDMJ + 10 wt.% GdCl$_3$ additions).

flaw recourses and thus damaged the mechanical properties and corrosion resistance seriously [12].

The compositions of these nonmetallic inclusions were analyzed by EDS as shown in Fig. 10. The results indicated that these nonmetallic inclusions were mainly MgO, chlorides and oxides of Gd and Y. The presence of Cl in inclusions, detected by EDS, demonstrated the existence of flux-inclusions. These flux-inclusions containing chlorides not only deteriorate the mechanical properties but also reduce the corrosion resistance of GW103K alloy.

In order to determine the removal efficiency of nonmetallic inclusions from Mg melt by refining process, the contents of inclusions in GW103K alloy were calculated using Leco image software. Table 2 shows the statistical volume fractions of the inclusions in alloy. The specimen refined by 5 wt.% GdCl$_3$ additions exhibited the lowest volume fraction of inclusions (0.84%). The effectiveness of the different purification methods on the removal of non-metallic inclusions can be expressed as the following sequence: JDMJ > JDMJ + 10 wt.% GdCl$_3$ additions > JDMJ + 5 wt.% GdCl$_3$ additions. This is also consistent with the refining results of mechanical and corrosion properties of GW103K alloy.

Table 2
Statistical volume fraction of inclusions in GW103K alloys refined with GdCl$_3$ additions.

	Number of fields	Average volume fraction (%)
JDMJ	30	2.16
JDMJ + 5% GdCl$_3$ additions	30	0.84
JDMJ + 10% GdCl$_3$ additions	30	1.02

3.5. Microstructure

Fig. 7 shows the microstructures of GW103K alloy (as-cast) refined with and without GdCl$_3$ additions. The black spots in the figures are nonmetallic inclusions. For the specimens refined with JDMJ + 5 wt.% GdCl$_3$ additions, the fraction of the inclusions is lower than in other specimens. It should be noted that the treatments with various GdCl$_3$ additions almost have no influence on the microstructures of the alloy, such as the eutectic phase morphology and the grain sizes. The compositions of phases of GW103K alloy unrefined (Fig. 11a) and refined with JDMJ + 5 wt.% GdCl$_3$ additions (Fig. 11b) were investigated using XRD. These results indicate that
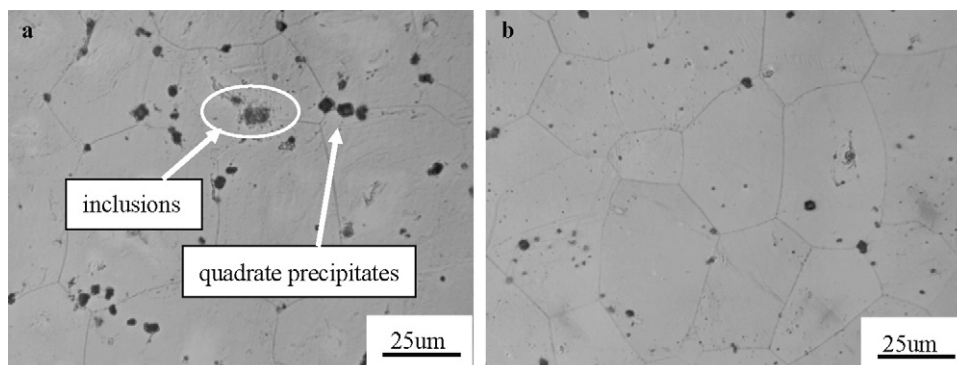

Fig. 8. Microstructures of GW103K alloy (T6 conditions) refined with different methods (a. unrefined, b. refined by JDMJ + 5 wt.% GdCl$_3$ additions).
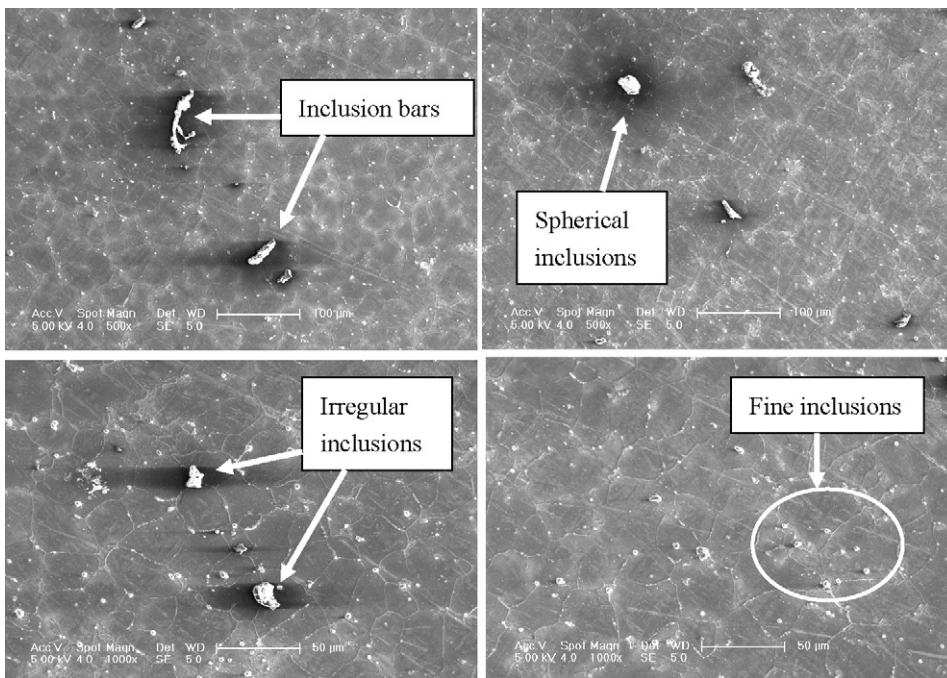
Fig. 9. Morphology and distribution of nonmetallic inclusions in GW103K alloy.

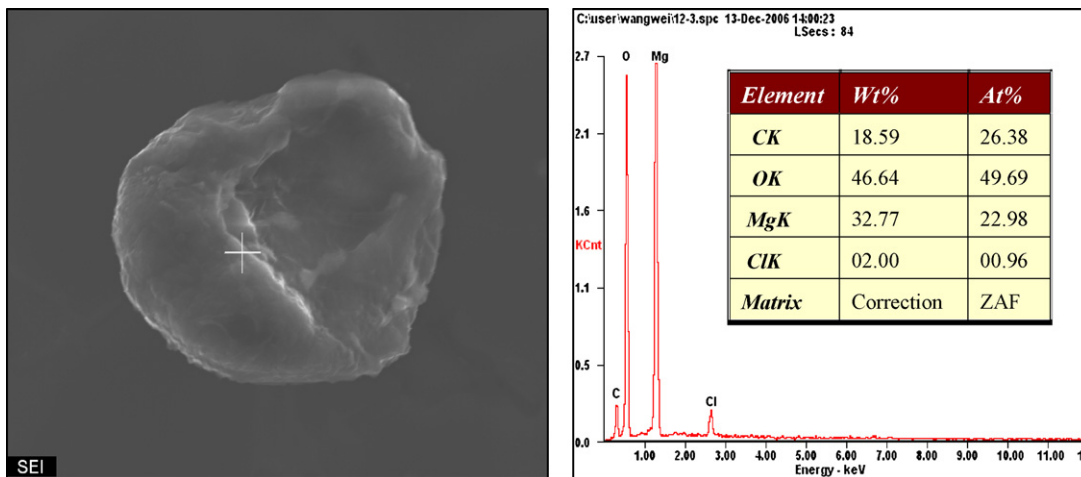| Element	Wt%	At%
CK	18.59	26.38
OK	46.64	49.69
MgK	32.77	22.98
ClK	02.00	00.96
Matrix	Correction	ZAF

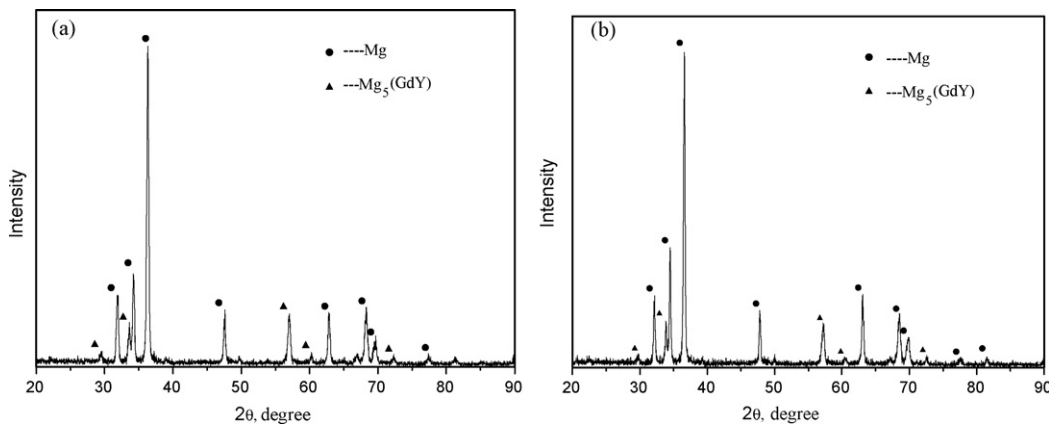**Fig. 10.** SEM photographs and EDS analyses of flux inclusion in GW103K alloy.

Fig. 11. X-ray diffraction (XRD) patterns of GW103K alloy refined by different treatments (a. unrefined, b. refined by JDMJ + 5 wt.% GdCl$_3$ additions).

the phase compositions of the alloy have not been changed, and are still consisted with matrix phase α-Mg and second phase Mg–Gd–Y compounds.

In T6 condition, the microstructures are different from as-cast condition as shown in Fig. 8. Nearly all the eutectic phase dissolved into the matrix only with some inclusions (circled in Fig. 8a, unrefined specimen) and quadrate precipitates remained. The dissolution of eutectic phase greatly impacts the mechanical and corrosion properties of GW103K alloy, as analyzed before. However, the fluctuation trends are very similar to as-cast condition.

The fracture surfaces of the specimens in as-cast condition after ambient temperature tensile tests are shown in Fig. 12. It is clear that the fracture pattern has not been changed greatly by the flux refining process. The fracture mechanisms are still quasi-cleavage crack. For the unrefined specimen, some big nonmetallic inclusions can be found on the fracture surface (see Fig. 12a).

3.6. Analysis of removing nonmetallic inclusions by flux

Generally, it is difficult to investigate the complicated cause of fluxes removing nonmetallic inclusions from melts by experiments. Therefore, we tried to analyze the cause via thermodynamic calculation.

The procedure of flux removing nonmetallic inclusions from melts can be divided in the following three steps: first, the collision between nonmetallic inclusions and molten flux; next, the nonmetallic inclusions adsorb flux; finally, the inclusion and flux drop together down to the bottom of the crucible. The second step is the restrictive link of the three.

The Gibbs free energy of nonmetallic inclusions adsorbed by flux can be expressed as:

$$-\Delta G = [\sigma_{m-i} - (\sigma_{f-i} + \sigma_{m-f})] \Delta \omega \tag{1}$$

where σ_{m-i}, σ_{f-i} and σ_{m-f} are the interfacial tension between melt, inclusion and flux and $\Delta \omega$ is the increment of surface area.

As can be seen from the Eq. (1), ΔG will be more negative with decreasing σ_{m-f} and σ_{f-i} while σ_{m-i} remain unchanged. This means

additions could reduce the surface tension of molten flux, and then decreases the interface tensions σ_{m-f} and σ_{f-i}. This makes ΔG (Eq. (1)) more negative and indicates that the removal of nonmetallic inclusions by flux could be easier to realize. However, too much GdCl$_3$ additions in flux could result in the increase of flux viscosity. This slowed down the sinking speed of the flux in the metallic melt. The flux and inclusions that did not sink to the bottom of the crucible remained in alloy as flux-inclusions. It should be noted that a molten flux is a considerably complex system. The effect of GdCl$_3$ additions on properties of flux, such as surface tension, viscosity, spreadability and structural of the molten flux, are still not clear. Further research works are necessary to elucidate its role.

3.7. Thermodynamic analysis for the suppression of Gd loss

In order to further explain how GdCl$_3$ suppresses the loss of Gd during refining process, we analyzed the mechanism from the aspect of thermodynamics. For the present study, the following chemical reaction should be taken into account.

$$3(MgCl_2) + 2[Gd] = 2(GdCl_3) + 3[Mg] \tag{2}$$

where the substances in roundparenthesis represent the substances in molten flux and the ones in squareparenthesis in Mg melts. Under standard conditions (1 atm and 298 K), the standard Gibbs free energy of the Eq. (2) could be obtained in terms of relative thermodynamic data [13].

$$\Delta G_1^0 = -79,810 \, \text{J/mol}$$

$\Delta G_1^0 < 0$ indicates that the reaction could occur spontaneously under standard conditions.

Under practical conditions, the change of Gibbs free energy of Eq. (2) should be calculated by Eq. (3).

$$\Delta G_1 = \Delta G_1^0 + RT \ln \frac{a_{Mg}^3 \times a_{GdCl_3}^2}{a_{MgCl_2}^3 \times a_{Gd}^2} \tag{3}$$

where a_{mg}, a_{MgCl_2}, a_{Gd} and a_{GdCl_3} are the activities of Mg, MgCl$_2$, Gd and GdCl$_3$ in the melt, respectively. The activities here are replaced by corresponding mole atomic concentration. For this experiment, $[Mg]_{mole}$, $[GdCl_3]_{mole}$, $[MgCl_2]_{mole}$ and $[Gd]_{mole}$ can be calculated as

$$[Mg]_{mole} = \frac{84.5/24}{84.5/24 + 11.4/157.25 + 0.125/263.75 + 1.116/95 + 3/89} = 0.966$$

$$[MgCl_2]_{mole} = \frac{1.116/95}{84.5/24 + 11.4/157.25 + 0.125/263.75 + 1.116/95 + 3/89} = 0.00323$$

$$[Gd]_{mole} = \frac{11.4/157.25}{84.5/24 + 11.4/157.25 + 0.125/263.75 + 1.116/95 + 3/89} = 0.0199$$

$$[GdCl_3]_{mole} = \frac{0.125/263.75}{84.5/24 + 11.4/157.25 + 0.125/263.75 + 1.116/95 + 3/89} = 0.00013$$

Substituting T with 1013 K, R with 8.314 J/mol K, then

$$\Delta G_1 = \Delta G_1^0 + RT \ln \frac{a_{Mg}^3 \times a_{GdCl_3}^2}{a_{MgCl_2}^3 \times a_{Gd}^2} = \Delta G_1^0 + RT \ln \frac{[Mg]_{mole}^3 \times [GdCl_3]_{mole}^2}{[MgCl_2]_{mole}^3 \times [Gd]_{mole}^2} = -20798.22 \, \text{J/mol}$$

it is easy for nonmetallic inclusions to transfer from magnesium melt to the flux. Once the nonmetallic inclusions move to the surface of the molten flux, the low σ_{f-i} allows for them to be captured by flux easily.

Fluxes containing less than 5 wt.% GdCl$_3$ were effective in removing nonmetallic inclusion, while the increase to 10 wt.% GdCl$_3$ had the opposite effect. It is supposed that a small quantity of GdCl$_3$

The negative value of ΔG_1 describes that the refining process with JDMJ + 5 wt.% GdCl$_3$ could not hold up the loss of Gd in alloy according to the reaction (1). But, compared with ΔG_1^0, the much higher value of ΔG_1 demonstrated that this process slows down the reaction velocity between Gd and MgCl$_2$ significantly, i.e. the loss of Gd in alloy was suppressed in a certain degree by adding GdCl$_3$ into Mg melt.
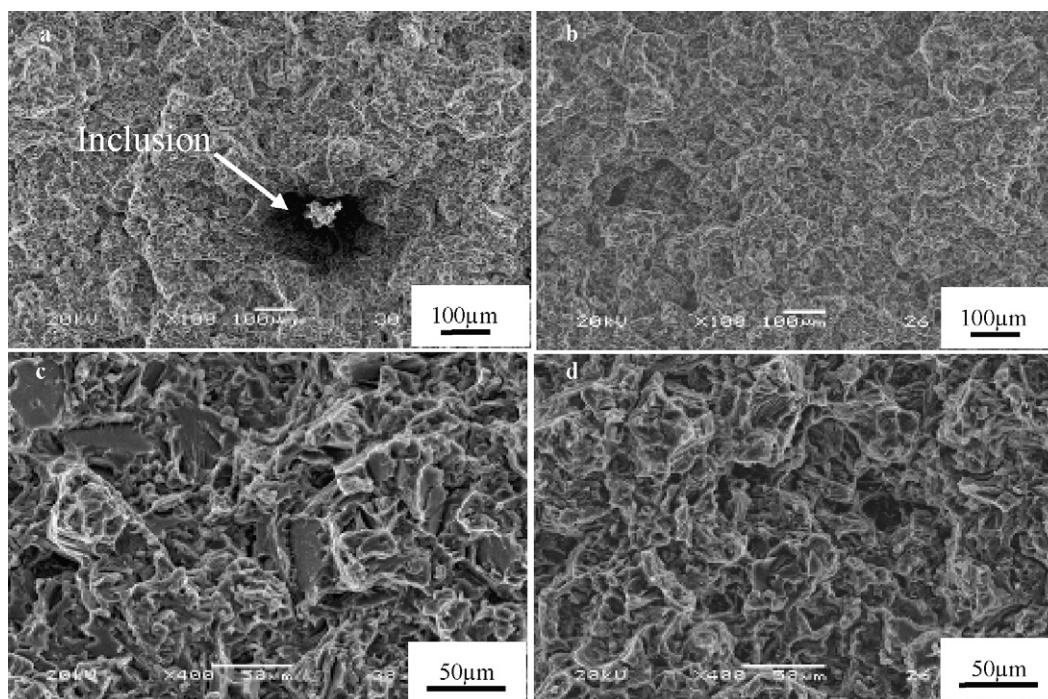
Fig. 12. Fractographs of tensile samples of GW103K alloy in as-cast condition (a, c. unrefined, b, d. refined by JDMJ + 5 wt.% GdCl$_3$).

4. Conclusions

Based on the experimental results obtained in this work, the following conclusions could be drawn:

(1) Introducing GdCl$_3$ into JDMJ flux is proved to be an effective measure to refine GW103K alloy melt. GdCl$_3$ additions can not only remove nonmetallic inclusions effectively but suppress the loss of Gd as well. The mechanism of this suppression effect was interpreted by thermodynamic calculation. The decline of the Gibbs free energy with the increase in the GdCl$_3$ additions slows down the reaction between MgCl$_2$ and Gd in melt.

(2) The refining process with JDMJ flux containing GdCl$_3$ can greatly improve the mechanical properties of GW103K alloy both in as cast and T6 conditions. The optimal content of GdCl$_3$ additions is 5 wt.%. σ_b, σ_s and δ reach the maximum value 201.51 MPa, 154.68 MPa and 2.5% for as cast specimens and 311.12 MPa, 241.17 MPa and 1.53% for specimens in the T6 condition.

(3) The corrosion rate of the alloy refined by JDMJ + 5 wt.% GdCl$_3$ declined to the minimal 1.1 mg cm^{-2} d^{-1} for as cast specimens and 0.677 mg cm^{-2} d^{-1} for specimens in T6 condition. However, addition of 10 wt.% GdCl$_3$ to the flux deteriorates the corrosion resistance of the alloy.

(4) The microstructure and fracture pattern of GW103K alloy are not changed by GdCl$_3$ treatments. The phase compositions of the alloy were still consisted with α-Mg matrix phase and second phase Mg–Gd–Y compounds, and the fracture mechanism remains quasi-cleavage crack.

References

[1] T. Honma, T. Ohkubo, K. Hono, Mater. Sci. Eng. A 395 (2005) 301–306.
[2] S. Schumann, Mater. Sci. Forum 488 (2005) 1–8.
[3] B. Rajagopalan, P.S. Mohanty, P.K. Mallick, Magnesium Technol. (2004) 131–136.
[4] M. Baghni, W. Yinshun, L. Jiuqing, Z. Wei, Trans. Nonferrous Met. Soc. China 14 (2004) 1–10.
[5] S.M. He, X.Q. Zeng, L.M. Peng, X. Gao, J.F. Nie, J. Alloys Compd. 427 (2007) 316–323.
[6] W.B. Du, Y.F. Wu, Z.R. Nie, X.K. Su, T.Y. Zuo, Rare Met. Mater. Eng. 35 (2006) 1345–1348.
[7] H.T. Gao, G.H. Wu, W.J. Ding, Y.P. Zhu, Trans. Nonferrous Met. Soc. China 14 (2004) 530–536.
[8] Z.H. Cheng, Magnesium Alloy, Chemical Industry Press, Beijing, 2004, pp. 64–70.
[9] C.Q. Zhai, W.J. Ding, X. Xu, Z. Deng, Z. Yu, Spec. Cast. Nonferrous Alloys 4 (2002) 292–295.
[10] H.T. Gao, G.H. Wu, W.J. Ding, L.F. Liu, X.Q. Zeng, Y.P. Zhu, Meter. Sci. Eng. A 368 (2004) 311–317.
[11] X.W. Guo, J.W. Chang, S.M. He, W.J. Ding, Electrochim. Acta 52 (2007) 2570–2579.
[12] K. Rohrig, 55th International Magnesium Conference, CO, USA, 1998, pp. 17–19.
[13] Y.J. Liang, Y.C. Che, X.X. Liu, Handbook of Inorganic Thermodynamic Data, North-East University Press, Shenyang, 1993.